RESERVES RE-ESTIMATION USING SCAL TO VALIDATE Sw MODEL FROM NEURAL NET PROCESSED OLD LOGS. LA CEIBITA FIELD, EASTERN VENEZUELA, CASE STUDY.

R. Panesso – PDVSA GAS, A. Quaglia – PDVSA GAS

ABSTRACT

La Ceibita field is located in the Oficina area in the Eastern Venezuela Basin. A total of 63 wells have been drilled, 48 (76%) with "old logs", prior to 1968, only 15 (24%) have logs between 1968 and 1982, including modern porosity logs. Production began in 1957, and 11 wells have been completed. A gas injection program was implemented in 1960 in order to maintain reservoir pressure. The purpose of the study was to generate a reliable Sw model using a methodology based on Neural Net technology, SCAL (Pc, wettability), rock type characterization, old and recent logs, production data, and, geological and reservoir information, in order to validate reserves and optimize exploitation plans.

The petrophysical characterization was aimed at the definition of rock types, which were classified based on pore throat radius estimated from mercury injection capillary pressure data. Pore throat radii corresponding to a mercury saturation of 45% represented the dominant interconnected pore system. Ranges of rock types from mega to nano porous were used to define flow units, with pore throat radius being the dominant control on permeability, flow capacity and water saturation.

Due to the lack of modern porosity logs it was necessary to apply alternate technologies such as Neural Net and modeling softwares to model resistivity curves and estimate porosity, which was related to core porosity. The detailed upscaling from core to log was performed using the relation found between pore throat radius obtained from cores and "true" formation modeled resistivity from electrical logs in the key well. Once porosity and resistivity were established, the Sw model was built and validated with SCAL data (Pc, wettability), fluid contacts and structural closure. One Acre/ft based calculations were made to re-estimate reserves, which in some cases reached up to 25% above the previous OOIP.

Detailed reservoir upscaling and the application of new technologies will always be more reliable as long as we demonstrate that uncertainty is diminished with real data, such as core, fluids and reservoir information. In this specific case the uncertainty that might be introduced by numerical processes as neural net technology and modeling software, was diminished using SCAL data such as capillary pressure and wettability.

INTRODUCTION

The studied reservoir is located in La Ceibita Field, Major Oficina Area, Eastern Venezuela Basin (Figure 1)**.** High pressures and high initial production rates, as well as a quick production decline characterize it.

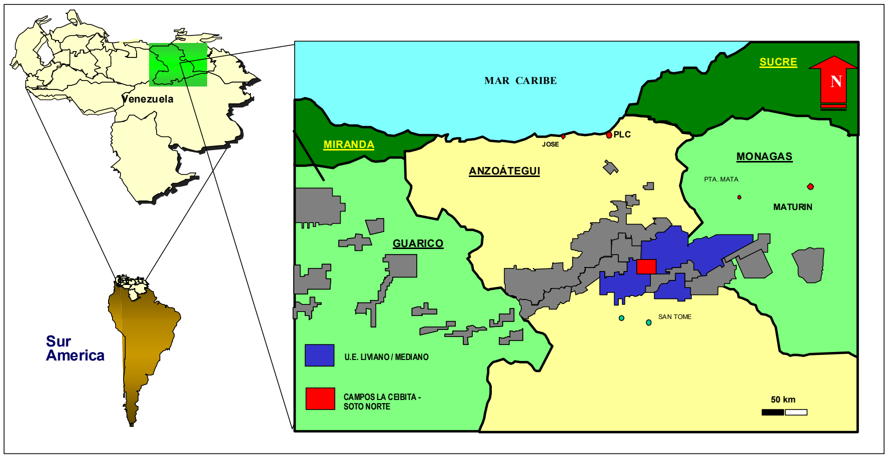

Figure 1- Geographic Location of La Ceibita Field

Rock type characterization was based on the integration of capillary pressure data, thin sections, SEM and XRD in core samples from key wells. This allowed the determination of the dominant pore throat radius of the interconnected porous system. For the sands studied, the dominant pore throat radius corresponds to a mercury saturation of 45%. This information was related to porosity and permeability based on Pittman's R45 equation, and allowed the classification of the rock according to pore throat size and definition of different rock types, from mega to nano porous.

RESISTIVITY MODELING

Resistivity inversion modeling was necessary because of the high proportion of logs from old resistivity tools. These logs rarely measure true in situ formation resistivities. Measurements from all resistivity tool configurations are inaccurate due to bed shoulder effects, apparent bedding dip angles, invasion effects, resolution limitations and wellbore environmental conditions (mud properties, hole rugosity, mudcake thickness).

Rt-Mod uses forward and inverse modeling methods to correct these effects, giving an accurate representation of true formation resistivity (Rt) at a bed boundary resolution of less than 2 feet for most logs.

The input data required for the resistivity modeling process are: deep & shallow resistivity curves, mud resistivity, borehole size information and tool transmitter-receiver spacing information.

Impact of Using Resistivity Modeling

Deep resistivity logging tools are used to measure formation resistivity, but they have poor vertical resolution. In thin beds, this results in bypassed pay and under estimation of reserves. Even in thick zones it is difficult to correctly identify reserves using conventional methods. Processing resistivity logs using Rt-Mod will significantly improve hydrocarbon reserve calculations and will help identify bypassed and untested pay zones.

Figure 2 shows the comparison between original and modeled resistivities, where it's noted that an "improvement" in resolution, minimizing the thin bed effect, results in increases in hydrocarbon saturation and therefore reserves.

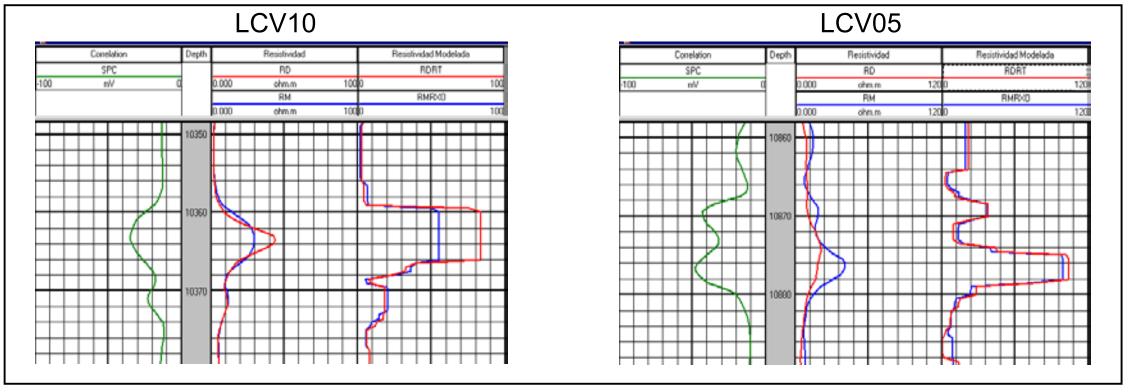

Figure 2 – Comparison between Original resistivity and Modeled resistivity

OLD LOGS POROSITY ESTIMATION FROM NEURAL NETWORK

Artificial Neural Networks 'learn' the nature of the dependency between input log and core data (the data that is abundantly available) and output curves (the curves you need), through a carefully selected and representative set of training examples. The Neural net uses a multi-layer backpropagation architecture to apply knowledge gained from training, allowing them to make new decisions, classifications, and predictions.

Due to the lack of porosity logs, a Neural Net was trained in order to generate a porosity curve from modeled resistivity and SP curves. Core porosity was also used as an important input. The neural Net was configured with two invisible layers (16 neurons each). It is important to mention that porosity ranges from this process were related, with acceptable correlation coefficient, to those ranges obtained from deterministic rock typing model, on wells with core and porosity log data available.

CALCULATION OF HEIGHT ABOVE FREE WATER LEVEL FROM CAPILLARY PRESSURE

The following map (Figure 3) shows two key wells, which have different predominant rock types and structural positions, representing not only estimated values of Height over FWL, but also validating, with small error bar, the OWC. Sw values for each Rock type sample, using modeled Rt and NN porosity, entered the Hg Pc chart to get Pc (lab) (Figure 4,5). Amott & USBM wettability and PVT analyses information played an important role in defining the assumptions necessary for estimations. This information indicates the strong water wettability tendency of the rock types used and some ranges of hydrocarbon densities, which go from 0.32 to 0.69 gr/cc, using an avg. value of 0.55 gr/cc to honor the predominant hydrocarbon component present in the reservoir.

In order to estimate the hydrocarbon column height, it was necessary to calculate Pc (field), to which the following equation was used:

$$\mathrm{Pc}_{\mathrm{field}} = \mathrm{Pc}_{\mathrm{lab}} \frac{\gamma_{field} \cos\theta_{field}}{\gamma_{lab} \cos\theta_{lab}} \tag{1}$$

Where: $\mathrm{Pc}_{\mathrm{field}}$ is the o-w capillary pressure (psi), $\mathrm{Pc}_{\mathrm{lab}}$ is the Hg capillary pressure (psi), γ_{field} is the Hg-air interfacial tension (dyne/cm), θ_{field} is the Hg-air contact angle (radians), γ_{lab} is the o-w interfacial tension (dyne/cm) and θ_{lab} is the o-water contact angle (radians).

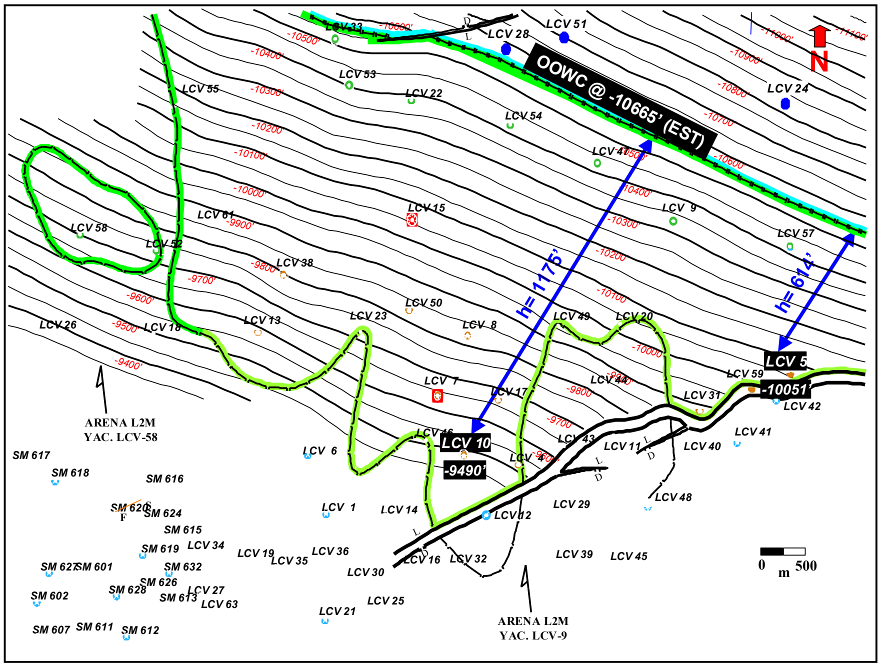

Figure 3- Structural position of LCV-05 and LCV-10 wells.

Hydrocarbon column height over FWL is determined using the following equation:

$$h = \frac{Pc_{field}}{0.433 * (\rho_{wet} - \rho_{non-wet})} \tag{2}$$

Where: h is the height above free water level (feet), $\mathrm{Pc}_{\mathrm{field}}$ is the oil-water capillary pressure (psi), 0.433 is a constant and is the gradient of pure water (psi/feet), ρ_{wet} is the wet phase density (gr/cc) and $\rho_{\mathrm{non\ wet}}$ is the non wet phase density (gr/cc).Equation 2 was used to build a Height-Sw chart, considering the rock types, which at the same time allows to identify the best estimate for hydrocarbon column height from a given Sw.

Well LCV-05

Table 1 – Parameters for studied reservoir estimations

Sw (%)	30	**γ_{field} (dyne/cm)**	50
Rock Type	Meso Porous (pore throat radii 0.5-2 microns)	**θ_{field} (degree/radians)**	10 / 0.17
γ_{lab} (dyne/cm)	480	**ρ_{wet} (gr/cc)**	1
θ_{lab} (degree/radians)	130 / 2.27	**$\rho_{\mathrm{non\ wet}}$ (gr/cc)**	0.55

From a given Sw (30% using Rt modeled) and the specific Pc test on the studied rock type, Pc_{lab} = 800 psi, (figure 4), then, using equations 1 & 2, Height above FWL is calculated. (h) = 655 ft. Figure 4 also shows a Height vs. Sw chart for Meso Rock Type which would allow the determination of the hydrocarbon column Height over FWL at any Sw for Meso rock in the studied reservoir. For this "Meso rock Type" Swi was estimated to be 25%, indicating a 5% difference in Sw with the LCV-5 well location. This difference is equivalent to 982 additional feet up dip, if one well should be at Swi conditions.

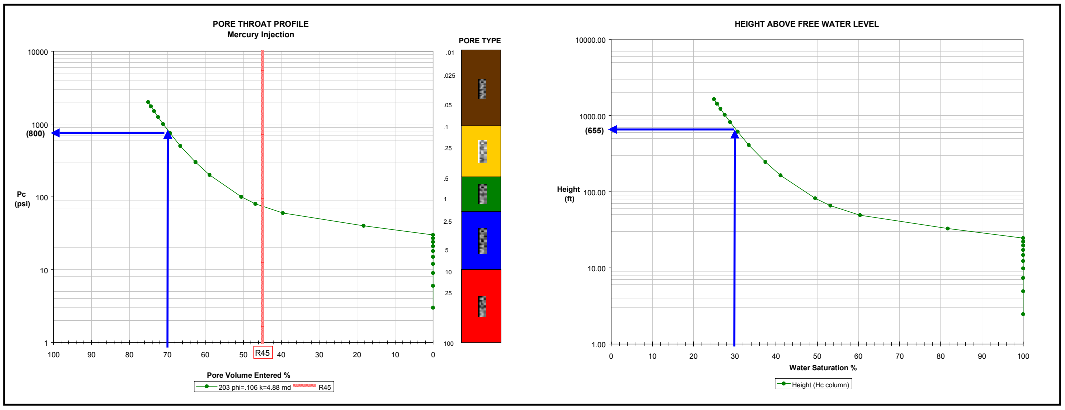

Figure 4 - Pc and Height vs Sw Chart of LCV-05 well.

<u>Well LCV-10</u>

Table 2 – Parameters for studied reservoir estimations.

Sw (%)	21	**γ_{field} (dyne/cm)**	50
Rock Type	Macro Porous (pore throat radii 2-10 microns)	**θ_{field} (degree/radians)**	10 / 0.17
γ_{lab} (dyne/cm)	480	**ρ_{wet} (gr/cc)**	1
θ_{lab} (degree/radians)	130 / 2.27	**$\rho_{non\ wet}$ (gr/cc)**	0.55

The second case tells from a given Sw (21% using Rt modeled) and the specific Pc test on the studied rock type, Pc_{lab} = 1400 psi, (figure 5), then, using equations 1 & 2 , Height above FWL is calculated. (h) = 1146 ft. Figure 5 also shows a Height vs. Sw chart for Macro Rock Type which would allow to determine hydrocarbon column Height over FWL at any Sw for Macro rock in the studied reservoir. For this "Macro rock Type" Swi was estimated to be 18%, indicating a 3% difference in Sw with the LCV-10 well location. This difference is equivalent to 491 additional feet up dip, if one well should be at Swi conditions.

There is a 5% average error in Height calculations between the ones measured from OWC in the map and those calculated from the PC derived chart. Besides that, an avg. of 25% increment in total reserves (OOIP) was obtained, using representative wells from the studied reservoir in La Ceibita Field.

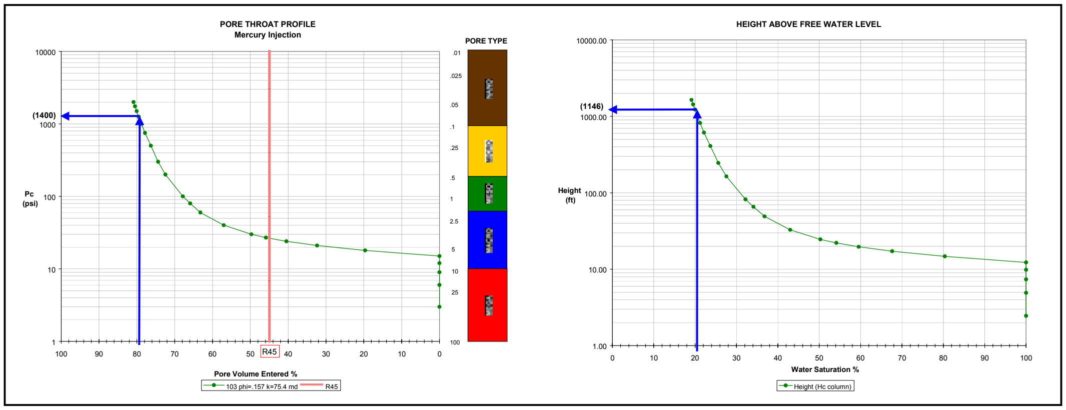

Figure 5- Pc and Height vs Sw Chart of LCV-10 well.

Table 3 – Comparison between different calculated hydrocarbon column heights and OOIP increments from the application of this methodology in La Ceibita Field.

Well	Sw with RT model	Rock Type	Pc (from Hg Injection) psi	h (from Structural Map) feet	h (from Capillary Pressure) feet	% Error	OOIP (before) bls/ac-pie	OOIP (after) bls/ac-pie	% Increment OOIP
LCV-05	0.30	MESO	800.00	614.00	655.00	-6.26	205.00	489.00	138.54
LCV-10	0.21	MACRO	1400.00	1175.00	1146.00	2.53	619.00	781.00	26.17
LCV-53	0.26	MEGA	300.00	259.00	245.00	5.71	582.00	863.00	48.28
LCV-22	0.36	MESO	360.00	282.00	294.00	-4.08	271.00	296.00	9.23
LCV-47	0.26	MACRO	300.00	241.00	246.00	-2.03	702.00	807.00	14.96
LCV-09	0.35	MESO	420.00	324.00	344.00	-5.81	447.00	508.00	13.65
LCV-57	0.26	MACRO	300.00	234.00	246.00	-4.88	515.00	633.00	22.91
LCV-38	0.28	MESO	1100.00	893.00	900.00	-0.78	423.00	611.00	44.44
LCV-07	0.21	MACRO	1200.00	1022.00	982.00	4.07	698.00	737.00	5.59

REFERENCES

1. Franklin, M., Resistivity/SP Modeling and Neural Network Synthesis of Log and Core Properties, Rocky Mountain Petrophysics, LLC, Aurora, U.S.A. 2001.
2. Hartmann, D. J., Petrophysical Integration, PDVSA, Workshop, Puerto La Cruz, Venezuela, 2000, Sections: 1-10.
3. Pittman, E. D., "Relationship of Porosity and Permeability to Various Parameters Derived From Mercury Injection – Capillary Pressure Curves for Sandstone", AAPG Bulletin, Tulsa, U.S.A., 1992, pp. 191-198.
4. Potter, G. F., Relative Permeability & Capillary Pressure, Amoco Exploration & Production Company, Tulsa, U.S.A., 1999, pp. 1-43.
5. Sneider, R. M., Sneider, J. S., Geoscience-Petrophysical-Petroleum Engineering Concepts to Improve Wellbore Evaluation & Hydrocarbon Recovery, Amoco Exploration & Production Company, Tulsa, U.S.A., 1999, pp. 1.1 – 1.43.
6. Tiab, D., Donaldson, E., Petrophysics, Gulf Publishing Company, Houston, U.S.A., 1996, pp.233-302.